An H minority heating regime in Tore Supra showing improved L mode confinement

G.T. Hoang, P. Monier-Garbet, T. Aniel, C. Bourdelle, R.V. Budny*, F. Clairet, L.-G. Eriksson, X. Garbet, C. Grisolia, P. Platz, J.C. Vallet

Association Euratom–CEA sur la Fusion,
Département de Recherches sur la Fusion Contrôlée,
CEA Cadarache, Saint-Paul-lez-Durance, France

* Princeton Plasma Physics Laboratory, Princeton University,
Princeton, New Jersey, United States of America

Abstract. Tore Supra experiments are at present devoted to the study of high density regimes with radiofrequency heating. Recently, an improved L mode confinement regime has been observed in plasmas heated by ion cyclotron hydrogen minority heating, at relatively high densities up to 80% of the Greenwald limit. The quality of energy confinement is as good as that of ELMy H mode. The main physical mechanism of this regime has not been clearly identified. However, some features very similar to those of previous improved confinement modes using neutral beam heating in other tokamaks have been observed.

1. Introduction

High density and high radiation regimes have been investigated for several years in tokamaks because they are considered to be a solution to the excessive heat load on the plasma facing components, particle control through pumping and thermalization of fast particles for the next tokamak generation. High energy confinement will also be required for fusion reactor operation. Nowadays, the attractive high radiation improved confinement regime (RI mode), discovered on TEXTOR [1], has been extensively studied in many tokamaks of various sizes such as TFTR [2] and DIII-D [3]. In these experiments, however, plasmas predominantly heated by NBI were used.

In Tore Supra (a major radius $R \leq 2.4$ m, a minor radius $a \leq 0.8$ m, a toroidal magnetic field $B_T \leq 4.2$ T and a plasma current $I_p \leq 2$ MA), recent experiments have been investigated with plasmas heated by ion cyclotron resonance minority heating (ICRH) only. The properties of the high density regime, in terms of confinement and stability, have been explored in steady state. Very encouraging results have been achieved. A confinement higher than L mode, with an energy confinement time close to that of ELMy H mode, has been observed. In spite of a moderate radiation fraction, these ICRH discharges have some features very similar to the results of the above mentioned machines and the improved ohmic confinement (IOC) regime in ASDEX [4].

This article is organized as follows. The experimental conditions are described in Section 2. In Section 3 global confinement and transport are analysed. Energy confinement is compared with that of the standard L mode regime. Comparisons of the confinement with the empirical predictions, using a wide data set, are discussed in Section 3. The dependences of the improvement factor upon the plasma density and the radiation fraction are also analysed. Section 4 reports the characteristic features of these discharges, such as the toroidal rotation and the peakednesses of the plasma density and current density. Finally, the conclusions are presented in Section 5.

2. Experiment

The experiments are performed in the limiter configuration. The plasmas are limited by a combination of the first inner wall and an outboard pump limiter: $R = 2.34$ m and $a = 0.78$ m. The plasma current ranges from 1.0 to 1.5 MA. A hydrogen minority on-axis heating scheme is used, at frequencies of 57 or 48 MHz, with the injected power P_{RF} varying from 2 to 9.5 MW, corresponding to a total power P_{tot} up to 10 MW. The toroidal magnetic field is fixed at 3.7 or 3.1 T to localize the absorption layer close to the magnetic axis. The working gas is either deuterium or helium. The density is raised by gas puffing to obtain the pre-programmed value (central line averaged density $\bar{n}_e \approx (4.2{-}5.2) \times 10^{19}$ m^{-3}). Usually, when ICRH power is applied the density

increases, reaching the preset value. The density is then maintained at this steady state value without gas fuelling. This differs from L mode discharges, in which gas injection is required during the additional heating phase in order to maintain the density at the pre-programmed value. Radiated power P_{rad}, measured by a bolometry diagnostic, increases with ICRH power, mainly due to intrinsic carbon and oxygen impurities. However, the fraction of radiation ($f_R = P_{rad}/P_{tot}$) decreases from the ohmic level reaching a value between 25 and 45%, depending on the plasma density and especially on the total power. The highest value, $f_R = 45\%$, corresponds to P_{tot} lower than 3 MW.

Good electron heating is observed in these discharges. Central temperature ($T_e(0)$) rose from 2 keV up to 5 keV (compared with 4 keV in the standard L mode discharge). Usually, for high current discharges, $I_p = 1.3$–1.5 MA, giant sawteeth appear with periods of 160–200 ms. The central ion heating is also more efficient than that in L mode discharges: $T_i(0)$ increased from 1.5 keV to more than 3 keV (compared with 2.2 keV in standard L mode discharges). Strong ion heating could be due to the high minority ion density. Indeed, the hydrogen concentration, defined as $C_H = n_H/n_e$ (n_H being the hydrogen density), is between 10 and 15% instead of less than 5% in the L mode discharges. Increase of minority concentration reduces the tail energy, which is favourable for balanced ion/electron heating. This is confirmed by a simulation using the PION code [5].

3. Confinement and transport analysis

In the following, the discharges described earlier will be compared with a series of discharges exhibiting standard L mode confinement. The L mode data set consists of various scenarios for plasma heating: either with ICRH H minority alone or with a combination of ICRH and drive LHCD. The discharges have been performed at the same plasma current, total injected power and electron density. For the L mode discharges the gas injection is usually switched on during the additional heating phase in order to reach the preset density. Conversely, in the improved confinement discharges, the gas fuelling is switched off during the ICRH pulse.

A comparison of an improved confinement deuterium discharge (shot TS23418) with the corresponding L mode discharge (shot TS25222) is shown in Fig. 1. Additional heating consists of 7 MW of ICRH in the H minority scheme (P_{tot} is approximately 7.5 MW) at $I_p = 1.5$ MA, $B_T = 3.7$ T, and a value for the safety factor at the edge $q_a = 3.7$. When the ICRH power is applied the density increases, due to deuterium desorption from the inner wall and the ICRH antennas. The central line density reaches the pre-programmed value of 7.5×10^{19} m^{-2} (corresponding to a line averaged density $\bar{n}_e = 4.75\times10^{19}$ m^{-3}, which is 60% of the Greenwald density limit [6]). Note that the pumping by the outboard limiter is not efficient in shot TS23418, while pumping is activated in the L mode case. For shot TS25222, the quantity of injected gas is reduced by a factor of 4, due to wall and outboard limiter pumping, whereas the gas valve is closed in shot TS23418 due to high wall saturation. The average effective charge Z_{eff} rises from 2 to 2.4 (2.3 in L mode shot TS25222) with the application of ICRH power, mainly due to an increase of carbon and oxygen impurities. Radiated power increases from 0.9 to 2.2 MW, but the fraction P_{rad}/P_{tot} drops from 60 to 30%.

The confinement of shot TS23418 is found to be improved. Both stored energy W_{tot} and electron energy W_e are approximately 1.4 times higher than those of L mode, shot TS25222. W_{tot} reaches 0.9 MJ, corresponding to an energy confinement time of about 120 ms. Observation of the same enhancement factors in the electron channel and in total energy suggests that ion confinement is also improved.

Figure 1 also shows a comparison of the confinement with the L mode predictions. For this comparison, we used the familiar scalings ITERL97-P [7] and Rebut–Lallia–Watkins [8], which are relevant to total confinement and electron energy content, respectively. Both scalings fairly well reproduce the L mode Tore Supra discharges, whose confinement exhibits a significant plasma density dependence [9]. The ITERL97-P and Rebut–Lallia–Watkins predictions are respectively given by

$$W_{tot}^{ITERL97\text{-}P} = 0.023\kappa^{0.64}R^{1.83}\varepsilon^{-0.06}I_p^{0.96}B_T^{0.03} \times n^{0.40}P^{0.27} \quad (1)$$

and

$$W_e^{RLW} = 2.6\times10^{-2}(\kappa a^2 R)^{11/12}I_p^{0.5}B_T^{0.5}n^{0.75}Z_{eff}^{0.25} + 1.2\times10^{-2}I_p\,P_{tot}\,Z_{eff}^{-0.5}(\kappa a^2 R)^{0.5}. \quad (2)$$

Analysis of a data set (more than 70 shots) gives an enhancement factor, $H_{ITERL97\text{-}P}$ with respect to ITERL97-P ranging from 1.4 to 1.7. The stored

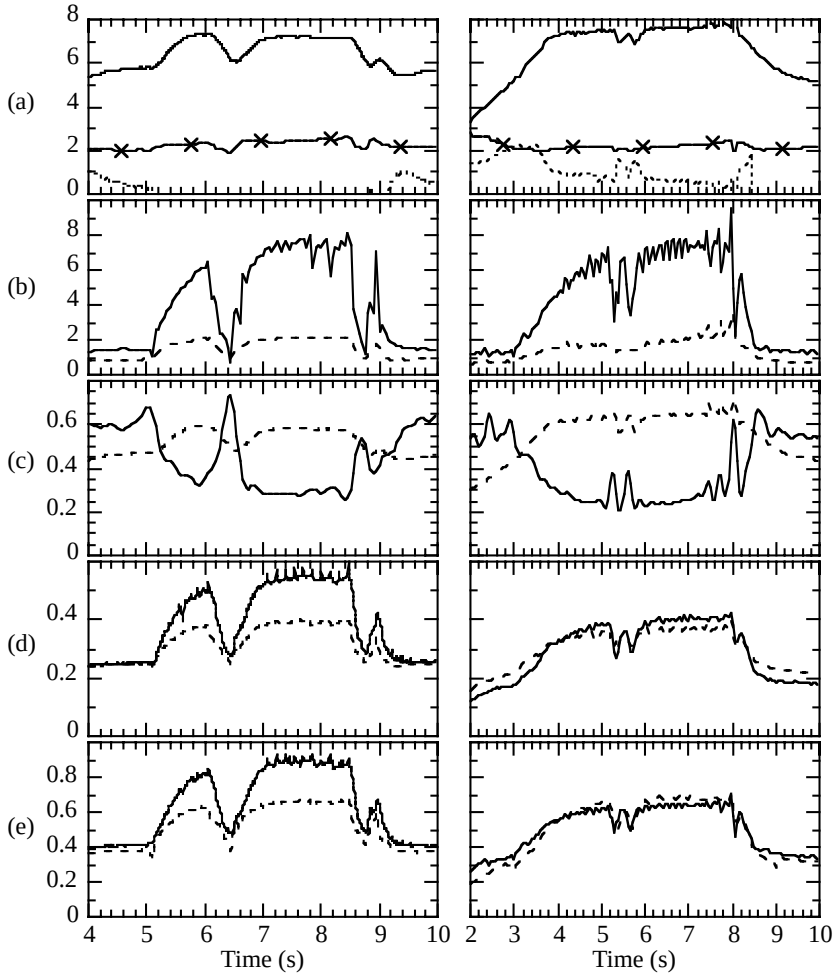

Figure 1. Comparison of an improved confinement discharge (shot TS23418, left hand side) and a standard L mode discharge (shot TS25222, right hand side), performed at a plasma current of 1.5 MA: (a) central line density in units of 10^{19} m^{-2} (full curves), averaged effective charge Z_{eff} (crosses) and gas injection in arbitrary units (dots); (b) total power (full curves) and radiated power (dashed curves), in megajoules; (c) radiated power fraction (full curves) and central line averaged density normalized to the Greenwald limit (dashed curves); (d) electron energy (full curves) and Rebut–Lallia–Watkins L mode scaling (dashed curves), in megajoules; (e) stored thermal energy (full curves) and ITERL97-P scaling (dashed curves), in megajoules.

energy versus ITERL97-P scaling is summarized in Fig. 2, in which L mode discharges are also shown for comparison. It is interesting to note that the confinement is very close to the prediction of ELMy H mode, as shown in Fig. 3. This figure shows a comparison with the ELMy H mode ITERH97-P scaling resulting from a fit of various tokamak data [10] given by

$$W_{tot}^{ITERH97\text{-}P} = 0.029\,\kappa^{0.92}\,M^{0.20}\,R^{2.03}\,\varepsilon^{0.19} \times I_p^{0.90}\,B_T^{0.20}\,n^{0.40}\,P^{0.34}. \quad (3)$$

A scan of ICRH power shows that the enhancement factor $H_{ITERL97\text{-}P}$ increases with P_{tot} (Fig. 4), indicating a power degradation weaker than that in the L mode regime. Figures 5(a) and (b) show the dependence of the improvement factor on plasma density normalized to Greenwald density. The $H_{ITERL97\text{-}P}$ factor is almost constant with increasing plasma density to 80% of the Greenwald limit (Fig. 5(a)). On the contrary, an increase of enhancement factor with density has been observed

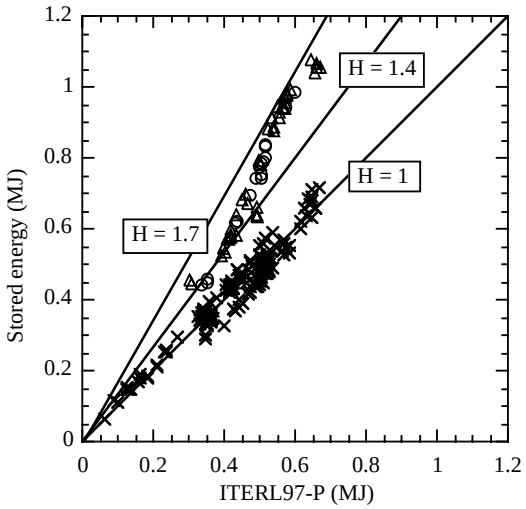

Figure 2. Stored thermal energy versus ITERL97-P prediction (circles, deuterium discharges; triangles, helium discharges; crosses, deuterium/helium L mode discharges).

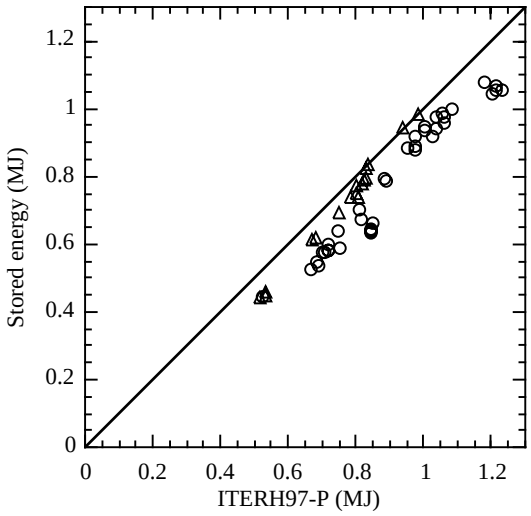

Figure 3. Stored thermal energy versus ITERH97-P prediction of thermal energy for ELMy H mode (circles, deuterium discharges; triangles, helium discharges).

in the RI mode of TEXTOR. The different behaviour of enhancement factor in these two tokamaks could be explained by the definition of the improvement factor using different scalings. Indeed, the ITERH93-P scaling for the ELM-free H mode [11] is used to define the enhancement factor in TEXTOR. The ITERH93-P prediction is given by

$$W_{tot}^{ITERH93\text{-}P} = 0.036\,\kappa^{0.66}\,M^{0.41}\,R^{1.79}\,\varepsilon^{0.11} \times I_p^{1.06}\,B_T^{0.32}\,n^{0.17}\,P^{0.33}. \quad (4)$$

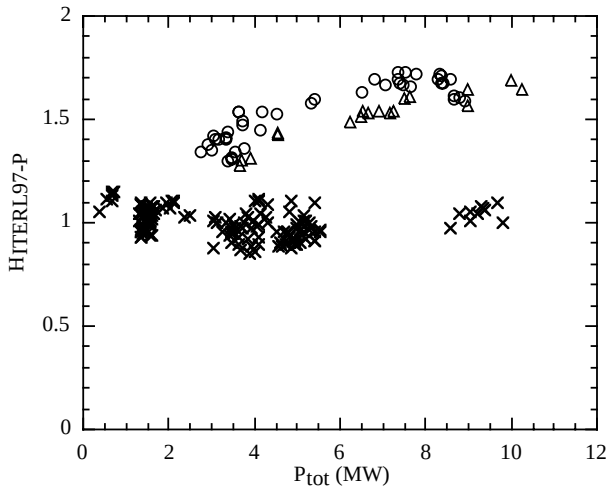

Figure 4. Enhancement factor with respect to the ITERL97-P prediction versus total input power (circles, deuterium discharges; triangles, helium discharges; crosses, deuterium/helium L mode discharges).

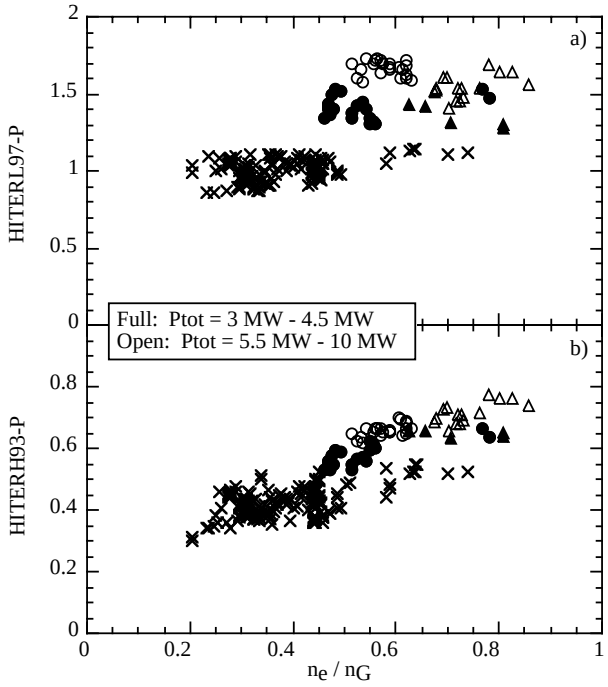

Figure 5. Enhancement factor versus plasma density normalized to the Greenwald limit (circles, deuterium discharges; triangles, helium discharges; crosses, deuterium/helium L mode discharges): (a) with respect to the ITERL97-P prediction, (b) with respect to the ITERH93-P prediction.

In Eq. (4) the density dependence is weaker than those in the scalings recently revised, either the L mode ITERL97-P (Eq. (1)) or the H mode

ITERH97-P (Eq. (3)). Using the enhancement factor definition of TEXTOR (e.g., with respect to ITERH93-P, $H_{ITERH93\text{-}P}$) for Tore Supra, we find a weak density dependence as shown in Fig. 5(b). The $H_{ITERH93\text{-}P}$ factor is found to vary approximately as $n_e^{0.3}$.

The confinement is not sensitive to the radiated power fraction, as shown in Fig. 6. In this figure, the weak decrease of the $H_{ITERL97\text{-}P}$ factor, with f_R being between 25 and 45%, is mainly due to the decrease of P_{tot}, since diminishing P_{tot} increases f_R and decreases $H_{ITERL97\text{-}P}$ (Fig. 4). To explore the high radiation regime, neon injection has been used during the improved confinement phase. In these experiments, at moderate RF power (3–4.5 MW), the fraction f_R is raised from 30 to 60% ± 10% by neon injection, but this does not affect confinement. It can be seen in Fig. 6 that for f_R higher than 50%, which corresponds to discharges with neon injection, the $H_{ITERL97\text{-}P}$ factor is maintained at the value of 1.4 previously observed without neon injection with a given total power in the range 3–4.5 MW. This feature differs from the results observed in other machines such as ISX-B [12], TEXTOR [13, 14], DIII-D [3], and JET [15]. On the one hand, impurity injection improved confinement in ISX-B, TEXTOR and DIII-D, and on the other hand, impurity injection degraded confinement in JET. These different experimental results could be explained by various experiment conditions such as plasma configuration (limiter or divertor), additional heating scheme or impurity rate (probably still low in Tore Supra).

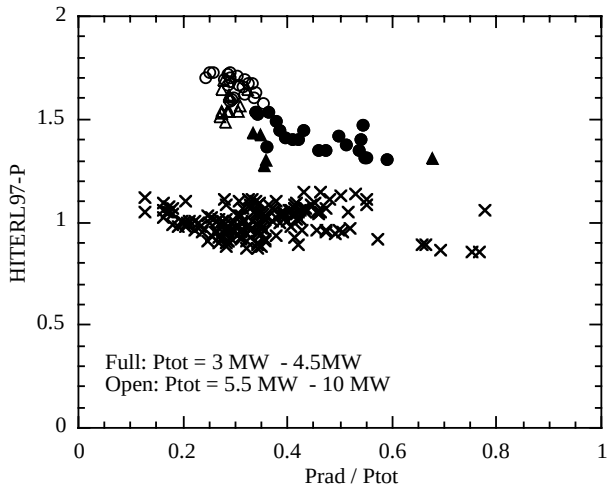

Figure 6. Enhancement factor with respect to the ITERL97-P prediction versus radiated power fraction (circles, deuterium discharges; triangles, helium discharges; crosses, deuterium/helium L mode discharges). The L mode discharges have been carried out without neon injection.

Transport analyses with the codes TRANSP [16] and LOCO [17] show a reduction of heat diffusivities from the L mode level. Profiles of the electron (χ_e) and one fluid effective (χ_{eff}) heat diffusivities of an improved confinement shot (No. TS23418) and an L mode shot (No. TS25222) are shown in Fig. 7. For these experiments, ion temperature profiles are not available. Only the central ion temperature is measured by the Doppler width of the Fe^{24+} ions from X ray measurement, and/or deduced from neutron rate. χ_i is predicted using a transport analysis. The same prediction is used for both L mode and improved confinement discharges. Predicted profiles for T_i are matched to be consistent with the time evolution of the central measured value and the global energy balance. Thus, the error bars of χ_i cannot be estimated. The uncertainties of χ_e and χ_{eff} are overestimated by varying predicted $T_i(r)$ from $0.3\,T_e(r)$ to $1.5\,T_e(r)$, while measured $T_i(0)$ is between 60 and 70% of $T_e(0)$. In our analyses, the ICRH power deposition is computed by the PION code [5]. In this code all the injected power is assumed to be absorbed within the plasma (via ion cyclotron damping, transit time magnetic pumping/electron Landau damping, etc.). Furthermore, the power deposition is coupled to a time dependent Fokker–Planck code, which calculates the distribution function of the resonating ions (on the number of flux surfaces) and the collisional transfer of power from these ions to the background plasma. The radial profiles of ICRH deposition are shown in Fig. 7, together with the radiation profile. Note that the high amount of power coupled to thermal ions in shot TS23418 is due to the high concentration of hydrogen minority (13% compared with 5% in shot TS25222). Heat diffusivities are determined by neglecting the radiation and convection in the power balance. This assumption affects weakly the analysis within the core region $r/a < 0.7$ since the radiation and convection powers are dominant only in the outer part of the discharge, typically for $r/a > 0.8$.

4. Characteristic features

During the improved confinement phase, both the electron density and the current density j profiles become more peaked, and an acceleration of the central toroidal rotation ($V_\Phi(0)$) from the counter-current direction to the co-current direction

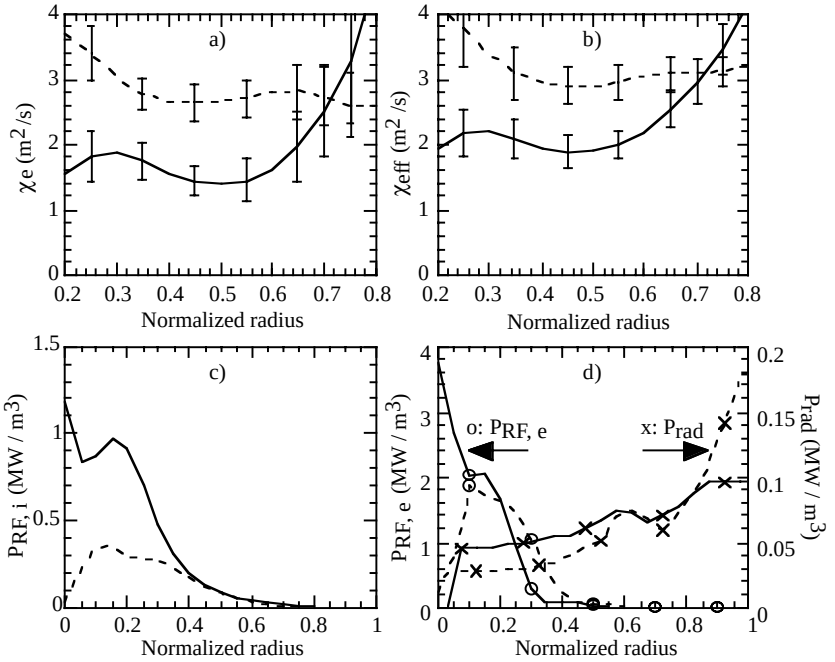

Figure 7. Transport analysis of the discharges in Fig. 1 (full curves, shot TS23418 at $t = 8$ s; dashed curves, L mode shot TS25222 at $t = 7.8$ s): (a) electron diffusivity χ_e, (b) one fluid effective diffusivity χ_{eff}, (c) radial profiles of RF power coupled to ions $P_{RF,i}$, (d) radial profiles of RF power coupled to electrons $P_{RF,e}$ and radiation power P_{rad}.

is observed simultaneously. These features are very similar to the various improved confinement regimes previously observed in ASDEX (improved ohmic confinement [18]), TEXTOR (RI mode [2, 3, 7, 8]) and DIII-D (RI mode [3]), JET [19], Alcator C-Mod [20].

The time evolution of density profile peaking of the discharge presented in Fig. 1 is shown in Fig. 8(a). The peaking factor is defined as the ratio $n_e(0)/\langle n_e \rangle$, where $\langle n_e \rangle$ is the volume averaged value. Figure 8(b) shows that the improved confinement discharge has a density profile more peaked than the L mode discharge. The difference in the gradient, mainly at the edge, can be attributed to the fact that the gas injection for the improved confinement shot is switched off because of the wall saturation status. The behaviour of the current density profile is illustrated in Figs 9(a) and (b). In Fig. 9(b), the j profile indicates a significant modification with an increase of magnetic shear in the region $0.2 \leq r/a \leq 0.8$. This is in agreement with the increase of the self-inductance l_i characterizing the current profile peaking (Fig. 9(a)). Here, j is obtained from Abel inversion of the measured Faraday rotation angle α_F, and from an equilibrium reconstruction using the IDENT-D code [21]. α_F is measured by a five chord infrared polarimeter ($R = 1.97$, 2.135, 2.3, 2.46 and 2.63 m), with a time resolution of 1 ms and a spatial resolution of 2 cm. The absolute error on the measurement of α_F is $\pm 0.25 \times 10^{-2}$ rad, corresponding to a systematic error in the range 5% (midradius) to 25% (centre). The correlation between the reduction of χ_e and the increased magnetic shear in the gradient zone is similar to that in improved confinement discharges observed in previous controlled current profile experiments on Tore Supra (the lower hybrid enhanced performance mode and the high bootstrap regime by fast wave electron heating) [8, 22].

Time traces of $V_\Phi(0)$, measured by the Doppler shift of the Fe^{24+} X ray line, are shown with the enhancement factor in Figs 10(a) and (b). In our collisional plasmas, the toroidal rotation speeds of the main ions and impurities are expected to be the same because of the strong parallel friction forces [23]. Neoclassical calculations indicate that this is indeed the case. Figure 10 shows an acceleration to the co-current direction during the improved confinement phase (Fig. 10(a)), whereas the standard

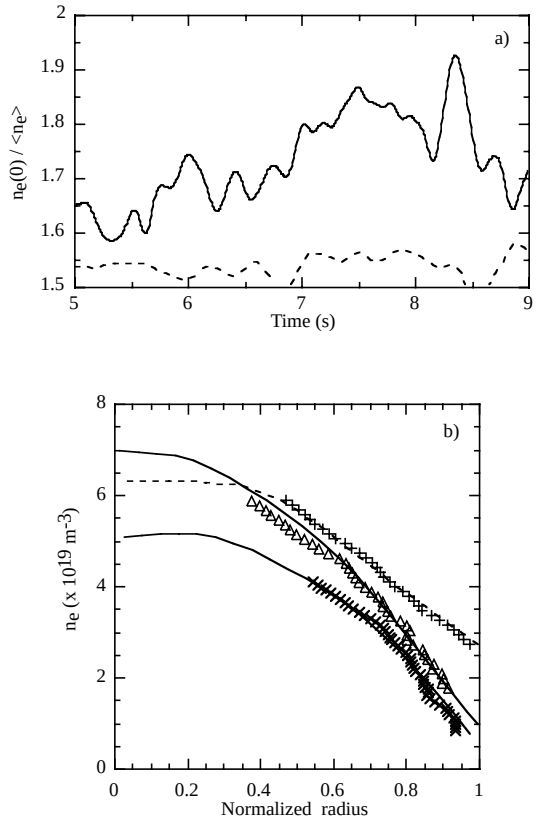

Figure 8. (a) Electron density profile peaking of the discharges shown in Fig. 1: shot TS23418 (full curve) and shot TS25222 (dashed curve). (b) Density profiles, measured by a reflectometry diagnostic, of shot TS23418 (triangles, measurement at $t = 8$ s; crosses, measurement before ICRH at $t = 4.5$ s) and of shot TS25222 (plus signs, measurement at $t = 7.8$ s). Full and dashed curves correspond to the fits of measured density from a twelve channel Thomson scattering diagnostic.

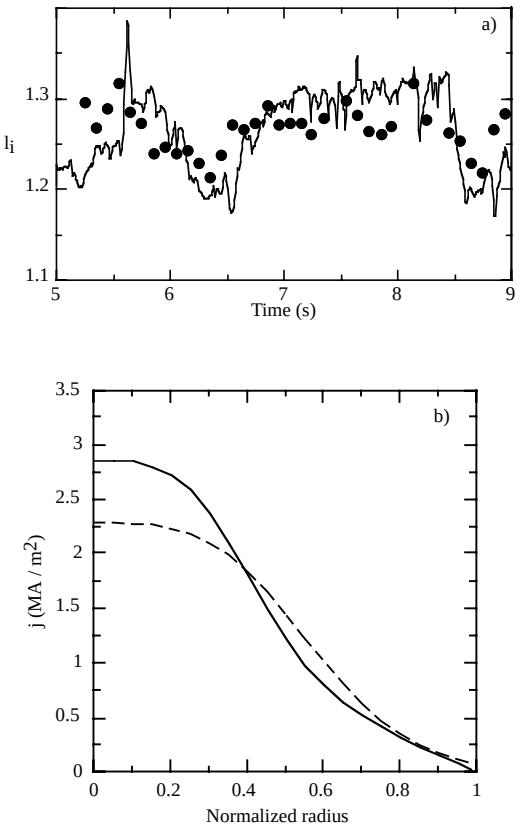

Figure 9. (a) Self-inductance of improved confinement shot, TS23418 (full curve, measurements; circles, IDENT-D equilibrium result). (b) Current density profiles from polarimetry measurements (full curve, shot TS23418 at $t = 8$ s; dashed curve, shot TS25222 at $t = 7.8$ s).

ICRH L mode plasma rotates in the counter-current direction (Fig. 10(b)). A more evident correlation between the change in $V_\Phi(0)$ and the improvement of confinement can be seen in Fig. 11, where the trajectories of some discharges are shown.

From these experimental observations, we are not presently able to identify the main physical mechanism of this improved confinement regime. More information, especially about the profiles of the poloidal and toroidal rotations, and the radial electric field E_r, is of course required. However, the inversion of the direction of the toroidal rotation from counter- to co-current direction and the density profile peaking suggest that E_r is modified. In addition, a possible increase of the ion pressure gradient (unfortunately not available) due to strong central ion heating can modify E_r. Both the modification of E_r and the increase of magnetic shear in the confinement region could contribute to the enhancement of transport. An analysis of impurity effects indicates a stabilizing effect on drift waves, but it is too weak to be the sole cause of transport reduction.

5. Summary and conclusion

A high L mode confinement has been observed on Tore Supra in relatively high density discharges with ICRH alone in the hydrogen minority scheme. A total stored energy slightly higher than 1 MJ has been obtained for 2 s with a total injected power of 10 MW. The energy confinement time of these discharges exceeds those of standard L mode discharges by a factor of up to 1.7. The improvement of confinement is observed in both electron and ion channels with reduced heat diffusivities. Balanced ion/electron heating is more pronounced than in standard L mode discharges, probably due to the

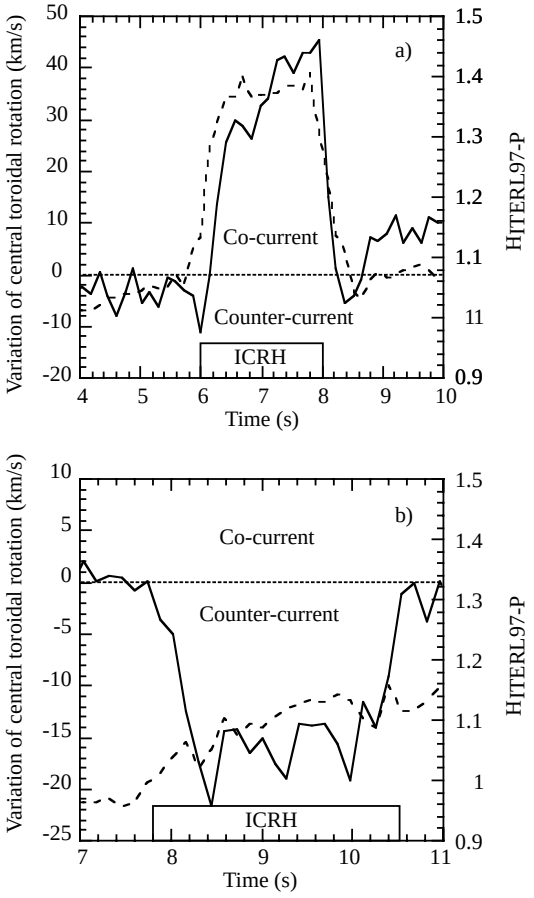

Figure 10. Variation of central toroidal rotation (full curve) and enhancement factor (dashed curve) for two helium discharges at I_p = 1.3 MA: (a) ICRH improved confinement described in this article, shot TS21044; (b) ICRH L mode, shot TS22642.

high minority concentration (10–15% instead of less than 5% in L mode). Furthermore, high confinement has been maintained for densities within the range 60–80% of the Greenwald limit, and for radiation fractions up to 60% (±10%).

Comparison of a wide database with the ITERL97-P scaling shows an enhancement factor $H_{ITERL97\text{-}P}$ ranging from 1.4 to 1.7. The confinement of these discharges is, moreover, close to that of the ITERH97-P scaling for ELMy H mode. Such a regime is very promising for alternative scenarios using ICRH in tokamak reactors, since a good confinement at high density improves the bootstrap current, which is necessary to sustain, together with external current drive methods, a full non-inductive current. High density operation is also favourable for improving the particle pumping and the radiation required for particle control and heat exhaust.

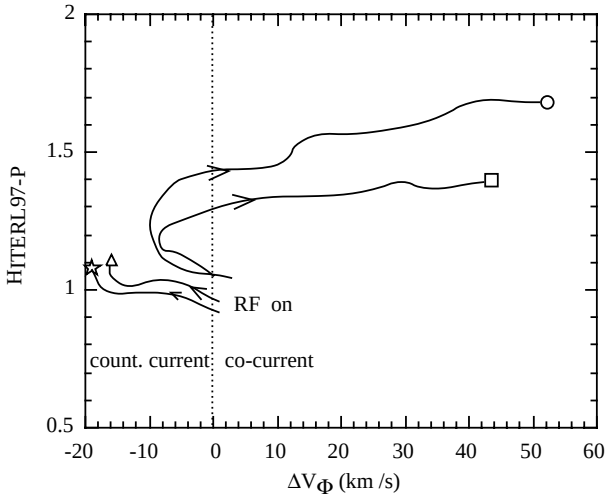

Figure 11. Evolution of the enhancement factor (with respect to the ITERL97-P prediction) with the toroidal rotation of four discharges (star, shot TS25222 in Fig. 1; circle, shot TS22805, a helium discharge similar to shot TS23418 shown in Fig. 1; triangle, shot TS22642 shown in Fig. 10; square, shot TS21044 in Fig. 10).

The present experimental results do not exhibit clearly any main physical mechanism of this regime. Some features, very similar to previous improved confinement modes using NBI in other tokamaks mentioned in this article, are, however, possible explanations:

(a) Increase of the magnetic shear in the confinement region (peaked current density profile),
(b) Modification of the radial electric field through increases of the peakednesses of the density profile and the toroidal rotation.

Acknowledgements

The diligent support of the Tore Supra team, in particular of the machine operation and RF groups, is gratefully acknowledged. The authors wish to thank Drs J. Ongena, A. Messiaen and B. Unterberg for useful discussions on RI mode in TEXTOR.

References

[1] Messiaen, A., et al., Phys. Rev. Lett. **77** (1996) 2487.
[2] Ongena, J., et al., in Controlled Fusion and Plasma Physics (Proc. 24th Eur. Conf. Berchtesgaden, 1997), Vol. 21A, Part IV, European Physical Society, Geneva (1997) 1693.

[3] Jackson, G.L., et al., Proc. J. Nucl. Mater. **380** (1999) 266.
[4] Söldner, F.X., et al., Phys. Rev. Lett. **61** (1988) 1105.
[5] Eriksson, L.-G., Hellsten, T., Willen, U., Nucl. Fusion **33** (1993) 1037.
[6] Greenwald, M., et al., Nucl. Fusion **28** (1988) 2199.
[7] Kaye, S.M., ITER Confinement Database Working Group, Nucl. Fusion **37** (1997) 1303.
[8] Rebut, P.H., Lallia, P.P., Watkins, M.L., in Plasma Physics and Controlled Nuclear Fusion Research 1988 (Proc. 12th Int. Conf. Nice, 1988), Vol. 2, IAEA, Vienna (1989) 191.
[9] Hoang, G.T., et al., Nucl. Fusion **38** (1998) 117.
[10] Cordey, J.G., ITER Confinement Database and Modelling Working Group, Plasma Phys. Control. Fusion **39** Suppl. 12B (1997) B115.
[11] Schissel, D.P., ITER H Mode Confinement Working Group, in Controlled Fusion and Plasma Physics (Proc. 20th Eur. Conf. Lisbon, 1993), Vol. 17C, Part I, European Physical Society, Geneva (1993) 1693.
[12] Lazarus, E.A., et al., Nucl. Fusion **25** (1985) 135.
[13] Messiaen, A., et al., Comments Plasma Phys. Control. Fusion **18** (1997) 221.
[14] Weynants, R.R., et al., Nucl. Fusion **39** (1999) 1637.
[15] Matthews, G.L., et al., Nucl. Fusion **39** (1999) 19.
[16] Budny, R.V., et al., Nucl. Fusion **32** (1992) 429.
[17] Harris, G.R., Capes, H., Garbet, X., Nucl. Fusion **32** (1992) 1967.
[18] Mertens, V., et al., Plasma Phys. Control. Fusion **32** (1990) 965.
[19] Eriksson, L.G., Righi, E., Zastrow, K.D., Plasma Phys. Control. Fusion **39** (1997) 27.
[20] Rice, J.E., et al., Nucl. Fusion **38** (1998) 75.
[21] Blum, J., et al., Nucl. Fusion **30** (1990) 1475.
[22] Hoang, G.T., et al., in Applications of Radiofrequency Power to Plasmas (Proc. 10th Top. Conf. Boston, 1993), AIP, New York (1994) 107.
[23] Kim, Y.B., Diamond, P.H., Groebner, R.J., Phys. Fluids B **3** (1991) 2050.

(Manuscript received 9 February 1999
Final manuscript accepted 14 February 2000)

E-mail address of G.T. Hoang: hoang@drfc.cad.cea.fr

Subject classification: B0, Te; F0, Te; F1, Te; F2, Te; G0, Te; G2, Te